

ANALYTICAL REPORT

[Ref.: AAR0955.A / 8 May 2018]



Paysage de Tiraspol (Tiraspol Landscape), 1905
Natalia Goncharova
Collection Museum Ludwig, Cologne, Inv. ML 1483

Art Analysis & Research Inc.
Ground Floor West, 162-164 Abbey Street, London SE1 2AN
T: +44 (0) 20 7064 1433
VAT Reg. No. 252 4541 22



Summary

A painting on canvas by Natalia Goncharova, *Paysage de Tiraspol (Tiraspol Landscape)*, belonging to the Museum Ludwig (reference: ML 1483), that has been dated to 1905 (it is unsigned and undated), was examined and analysed by Art Analysis & Research, Ltd. in cooperation with the Museum Ludwig, and funded through a grant from The Russian Avant Garde Research Project (RARP). This artwork formed a part of a group of fourteen well-provenanced paintings by the Russian artist couple Natalia Goncharova and Mikhail Larionov, held in the collection of the Museum Ludwig that comprised the focus of this work. The goal set for this research was to investigate these paintings in order to characterise similarities and differences, with the objectives of 1) providing detailed studies of the specific paintings, 2) obtaining wider information on the artists' methods, 3) defining a blueprint for promising methodologies to develop further on other works by these artists and with an aim of applying such information in support a *catalogue raisonné*, and 4) creating the foundation for applying similar methodologies and techniques to other artists of the genre. To this end, each of the paintings are described in individual reports (as here) accompanied by a summary report under separate cover. The results of the program of examination, material analysis and technical imaging will be set out herein.



Contents

Summary	2
Tables, Figures and Plates.....	4
A. Introduction.....	6
B. Examination, imaging and analysis of the images	7
B.1 Methodology	7
B.2 General observations	7
B.3 Imaging.....	8
B.3.i Photography with ultraviolet illumination	8
B.3.ii Surface conformation	8
B.3.iii Short-wave infrared (SWIR).....	9
B.3.iv X-radiography and weave analysis	9
C. Sampling and analysis	10
C.1 Introduction	10
C.2 Support	11
C.3 Radiocarbon dating.....	11
C.4 Ground.....	11
C.5 Underdrawing.....	12
C.6 Paint layers: Pigments	12
C.7 Paint layers: Binding media	12
C.8 Stratigraphy	12
D. Discussion of the findings.....	13
D.1 Support, ground and preparatory work	13
D.1.i The support	13
D.1.ii Priming.....	14
D.1.iii Underdrawing	14
D.2 Paint, pigments and binding media	14
D.2.i General observations.....	14
D.2.ii Paint: pigment and binding medium	15
D.2.iii Materials analysis and implications for dating	16
E. Conclusions	17
F. Acknowledgements.....	18
G. Appendices.....	19

App.1 Sampling and sample preparation	19
App.1.i Sampling	19
App.1.ii Cross-sectional analysis	20
App.2 Materials analysis summary results	20
App.2.i SEM-EDX, Raman microscopy and PLM analysis	20
App.2.ii Fourier Transform Infrared Spectroscopy-Attenuated Total Reflectance (FTIR-ATR)	22
App.2.iii. Gas Chromatography-Mass Spectrometry (GCMS) Analysis.....	24
App.2.iv SYPRO [®] Ruby protein staining	24
App.2.v. Canvas fibre identification	24
App.2.vi. Radiocarbon measurement	25
App.3 Imaging methods	27
App.4 Plates	28
App.5 Cross-sections	43

Tables, Figures and Plates

Table App.1.i Samples taken for analysis	19
Table App.2.i Analytical results SEM-EDX, Raman Microscopy and PLM	20
Table App.2.ii Summary results from FTIR	22
Table App.2.iii. Summary results from GCMS	24
Table App.2.iv. SYPRO [®] Ruby stain results for 955.A, Sample [7].....	24
Table App.2.v. Canvas fibre identification, Sample [14]	24
Table App.2.vi. Radiocarbon measurement.....	26
Plate 1. Natalia Goncharova, Paysage de Tiraspol (Tiraspol Landscape), 1905, collection Museum Ludwig: Inv. Nr. ML 01483. Recto, visible light.	28
Plate 2. Natalia Goncharova, Paysage de Tiraspol (Tiraspol Landscape), 1905, collection Museum Ludwig: Inv. Nr. ML 01483. Recto, UV light.	29
Plate 3. Natalia Goncharova, Paysage de Tiraspol (Tiraspol Landscape), 1905, collection Museum Ludwig: Inv. Nr. ML 01483. Recto, oblique illumination.....	30
Plate 4. Natalia Goncharova, Paysage de Tiraspol (Tiraspol Landscape), 1905, collection Museum Ludwig: Inv. Nr. ML 01483. Recto, 3D laser scan.....	31
Plate 5. Natalia Goncharova, Paysage de Tiraspol (Tiraspol Landscape), 1905, collection Museum Ludwig: Inv. Nr. ML 01483. Verso, visible light.	32
Plate 6. Natalia Goncharova, Paysage de Tiraspol (Tiraspol Landscape), 1905, collection Museum Ludwig: Inv. Nr. ML 01483. Verso, UV light.....	33
Plate 7. Natalia Goncharova, Paysage de Tiraspol (Tiraspol Landscape), 1905, collection Museum Ludwig: Inv. Nr. ML 01483. Recto, SWIR image.	34

Plate 8. Natalia Goncharova, Paysage de Tiraspol (Tiraspol Landscape), 1905, collection Museum Ludwig: Inv. Nr. ML 01483. Recto, SWIR image, detail. No underdrawing or pentimenti are visible; instead the thin, free nature of the brushwork may be seen.	35
Plate 9.a Natalia Goncharova, Paysage de Tiraspol (Tiraspol Landscape), 1905, collection Museum Ludwig: Inv. Nr. ML 01483. X-ray image.	36
Plate 9.b The X-ray image before digital compensation for the stretcher bars.	36
Plate 10.a Maps showing variation in canvas thread angle.	37
Plate 10.b Histogram of horizontal thread (in this case related to the warp) count readings.	38
Plate 10.c Histogram of vertical thread count readings (in this case related to the weft).	38
Plate 10.d Table of thread count data (threads per centimetre)	38
Plate 11.a Detail of canvas, verso.	39
Plate 11.b Detail of canvas, right tacking margin, showing selvedge, right, along top edge.	39
Plate 11.c Detail of canvas, bottom tacking margin, showing selvedge.	39
Plate 12.a Macro detail of the lead white-based priming on the canvas, recto.	40
Plate 12.b Higher magnification of the ground, as above.	40
Plate 12.c Detail of cracks in the painting, showing the effect of the granular ground on the paint surface.	40
Plate 13.a Macro detail, showing brushwork with a brush loaded with several colours.	41
Plate 13.b Detail of surface texture.	41
Plate 13.c Macro detail of a tree, background. Paint applied wet over dry.	41
Plate 14. Image showing approximate location of samples taken for materials analysis.	42
Plate 15. Cross-section, Sample [7].	43
Plate 16. Cross-section, Sample [7], stained with SYPRO [®] Ruby.	43
Plate 17. Cross-section, Sample [7].	44
Plate 18. Cross-section, Sample [9].	44
Plate 19. Cross-section, Sample [9].	45

A. Introduction

The painting known as *Paysage de Tiraspol* ('*Tiraspol Landscape*'; **Plate 1**) by the artist Natalia Goncharova (1881-1962), a work on canvas measuring 705 mm high by 890 mm wide, is now part of the collection of the Museum Ludwig, Cologne (Inv. ML 01483). It is unsigned and undated; a date of 1905 has been proposed for its creation. It has been examined as part of a larger technical study of fourteen paintings by Goncharova and Mikhail Larionov in the Museum Ludwig, as part of a project funded through a grant from the charity the Russian Avant Garde Research Project (RARP). The project goal has been to generate detailed technical profiles on authentic paintings by Goncharova and Larionov to expand the data available for art historical study and technical characterization of their work¹; consequently, fourteen well-provenanced paintings by the Russian artist couple held in the collection of the Museum Ludwig were thoroughly examined and analysed². The short-term goal of the project was to define a blueprint for promising routes of research to develop further on other works by these artists and with a long-term goal of contributing such information to support a technical *catalogue raisonné*; these recommendations are laid out in a summary report³.

The information in this report therefore provides a detailed technical and material account of the painting. In addition, this is considered in light of the conservation history and provenance information relating to the painting, held by the Museum Ludwig; the supplementary reports produced by Verena Franken in the course of her work on the RARP project summarises this material⁴. Some of the information concerning examination of the painting has been included here, as relevant, as are a representative selection of the extensive documentation photographs she made.

The structure of this report is as follows. First, the primary findings of the visual examination and technical imaging will be described in **Section B**.

¹ There is limited specific information available. This includes: Rioux, J.-P.; Aitken, G.; Duval, A. 'Étude en laboratoire des peintures de Gontcharova et Larionov', pp. 220-223. In: *Nathalie Gontcharova, Michel Larionov* [exh. cat.], Éditions du Centre Pompidou: Paris (1995). Rioux, J.-P.; Aitken, G.; Duval, A. 'Matériaux et techniques des peintures de Nathalie S. Gontcharova et Michel F. Larionov du Musée national d'art moderne', *Techne* 8 (1998) 7-32. Gallone, A. 'Œuvres de Michel Larionov et Nathalie Gontcharova: Analyse de la Couleur', *Le dessin sous-jacent la technologie dans la peinture: Colloque XI 14-16 septembre 1995*, R. Van Schoute and H. Verougstraete (eds), Louvain-la-Neuve (1997) pp. 137-141, Pl. 74-76.

² These include: Natalia Goncharova: *Paysage de Tiraspol (Tiraspol Landscape)*, 1905, ML 01483; *Rusalka*, 1908, ML 1304; *Still Life with Tiger Skin*, 1908, ML 1305; *The Jewish Family*, 1912, ML 1369; *The Orange Seller*, 1916, ML 1484; *Portrait of Larionov*, 1913, ML 1319.

Mikhail Larionov, *Still Life with Coffee Pot*, c. 1906, ML 01486; *Still Life*, c. 1907/1912, ML 1487; *Still Life with a Crayfish (Nature morte à l'écrevisse)*, c. 1907, ML 1331; *Portrait of a Man (Anton Beswal)*, c. 1910, ML 1306; *Rayonism, Red and Blue (Beach)*, 1911, ML 1333; *Saucisson et maquereau rayonnists (Rayonistic Sausage and Mackerel)*, 1912, ML 1307; *Venus*, 1912, ML 1332; *Rayonistic Composition*, inscribed 1916, ML/Z 211/134.

³ *Summary Report of the RARP Goncharova/Larionov Project, with the Museum Ludwig*, Art Analysis & Research Inc. (2017).

⁴ See reports: *AAR0955.A ML 1483 Conservation*, Franken, V. 'Report on the examination of the painting *Landscape of Tiraspol* (1905) by Natalia Goncharova' (2017a) and *AAR0955.A ML 1483 Archives*, Franken, V. 'Report on the content of the Museum Ludwig archives, concerning the painting *Landscape of Tiraspol* (1905) by Natalia Goncharova' (2017b).

Materials analysis on micro-samples taken for pigment and binding medium identification and cross-sections is described in **Section C**.

Inferences drawn regarding the painting on the basis of these investigations will be discussed in **Section D**.

The methodologies and protocols used in each case may be found described in the general **Protocols** supplement, appended to this series of reports.

B. Examination, imaging and analysis of the images

B.1 Methodology

The painting was initially examined visually under normal lighting conditions and with ultraviolet light (UV), then with a stereo binocular microscope.

A range of technical imaging techniques were also employed (**Appendix 3**), generating a variety of images and imaging datasets⁵. These are presented as follows:

- High-resolution visible colour (**Plates 1, 5**);
- UV luminescence (**Plates 2, 6**);
- Oblique illumination (**Plate 3**);
- 3D laser surface scanning (**Plate 4**);
- Short-wave infrared (SWIR), 1600-2500nm (**Plates 7, 8**);
- X-radiography (**Plates 9a, b**).

Additionally, weave analysis (including thread counting) was conducted on the basis of the X-radiograph (**Plates 10.a-c**). Some exemplar images recorded as part of the surface microscopy and macrophotography are also reproduced here (**Plates 11-13**).

The imaging revealed a range of aspects regarding the use of materials, structure and technique of production of the painting that are complementary to the visual observations made. Consequently, specific observation will be made to each in this section regarding the interpretation of these specific forms of analysis, while a summary overview in the context of the painting technique is presented in **Section D**, below.

B.2 General observations

The painting is executed on canvas, which has not been lined, so that both the recto and the verso of the artwork could be studied. It is not, however, on its original stretcher, having been restretched

⁵ Additionally, a visible-NIR multispectral dataset was collected to examine its suitability for study of paintings of Goncharova and Larionov. As it did not offer information significantly different or superior to that derived by the SWIR imaging, this has not been otherwise reproduced or further analysed here but is available for extramural studies in the future.

onto a newer secondary support. The painting is in good condition, with only minor, localised retouching where there have been small losses of paint, particularly along the upper edge.

B.3 Imaging

Each form of imaging offers different types of insight into the various material aspects of the painting. The most relevant are introduced, in brief, here.

B.3.i Photography with ultraviolet illumination

Excitation by ultraviolet (UV) light can induce luminescence⁶ in some materials, commonly seen as a weak re-emission of light in the visible region. Many natural varnishes have this property, emitting a characteristic weak greenish luminescence. While some pigments (notably zinc white and certain 'lake' pigments) are also active in this way, paints otherwise often do not luminesce. Because of the luminescence of varnishes, which are typically applied as a continuous coating across the surface of a painting, this can provide a means of determining if any disturbance has occurred, such as partial cleaning of the surface or addition of later restoration, where the changes show in contrast to the luminescent areas. Consequently, UV light is commonly used to reveal the presence of retouching. When paintings are not varnished, as is the case here, differences between the colour of the luminescence of the different paints and any added retouching paints can also indicate later stages of intervention (**Protocol 3.2** and **Plate 2**).

In the UV image of this work, small dark areas representing retouched losses of paint may be noted along the upper and lower edges of the art work. No strong luminescence was noted from any of the original paints.

B.3.ii Surface conformation

Two techniques for examination of the surface structure of the painting were used: photography under oblique illumination and 3D laser scanning. While the former may be the more familiar of the two as a physical examination technique, both essentially provide a means of elucidating paint texture and object deformations, either by recording shadowing, or through direct measurement of surface height. Of the two, 3D laser scanning offers important advantages in terms of being more replicable in the future (to support longer-term conservation assessments for example) and as a numerical dataset that can be studied visually and algorithmically for diagnostic features of technique. Imaging of the painting using oblique illumination, as well as 3D laser surface scanning (see **Protocol 3.3**), served to reveal two kinds of textural features that are particularly evident in this painting. The most visually dominant is the narrow, roughly vertical, banding, essentially an oriented crack network with concave distortion of the paint film in between. The underlying cause for this may have been

⁶ Commonly referred to as 'UV fluorescence', the word *luminescence* is used here as a broader term that may encompass not only fluorescence phenomena (prompt re-emission of light), but also phosphorescence (slow re-emission of light due to transition via forbidden quantum states). In both cases emission is typically at longer wavelengths than the excitation; here, the excitation is in the UV to blue part of the spectrum (hence 'UV'; in practice, so-called UV-A) and emission in the visible region.

rolling of the painting, although the inter-crack distance is relatively small for this⁷. This distortion is also visible on the verso of the painting.

Impasto arising from the brushwork is indicative of a fluid application of paint, with distinct build-up along edges of colour areas. For example, the lower left form of the corner of the field is effectively outlined by soft ridges of paint, as are the distant hills and trees of the background landscape.

The painting has been relatively recently re-stretched; consequently, there are no significant features arising from defective mounting to the secondary support.

B.3.iii Short-wave infrared (SWIR)

The interest in technologies capable of imaging artworks past the red end of the visible spectrum, in the ‘near’ (‘NIR’) or short-wave (‘SWIR’) infrared regions, has primarily developed out of the long-standing application to reflectography, exploiting the phenomenon of variable transparency of paint films at different wavelengths to enable visualisation of features lying beneath the surface. Imaging of underdrawing has been a major contribution to the study of authorship in paintings, permitting a fuller comprehension of artists’ working practices and extending the evidence used in attribution questions. Practical experience (as well as theoretical consideration) has shown that deeper IR cameras can confer additional benefits in terms of penetration to underlying layers; consequently, a system capable of operating in the SWIR region was used here (see **Protocol 3.4**).

In the IR image (**Plates 7-8**), no discrete underdrawing can be seen. However, this does not necessarily mean that no underdrawing is present; as imaging of other paintings examined in this project revealed, underdrawings in friable charcoal or dilute carbon black paint were not usually resolved, although examination at magnification showed its presence. The reason for the lack of resolution in IR lies in a number of factors, probably a combination of the thin and diffuse distribution of the material and the IR blocking properties of the thick overlying layers of paint. Thus, in this particular case, the presence or absence of an underdrawing cannot be ascertained with certainty; the canvas was densely covered with paint, allowing for very limited opportunity to find underdrawing in the gaps between adjacent areas of colour.

B.3.iv X-radiography and weave analysis

X-radiography shows internal structures in paintings because the transmitted X-rays are blocked to different degrees by virtue of the inherent absorption and thickness variations of the constituent materials. For example, pigments based on lead (such as ‘lead white’) stop the passage of X-rays more effectively than materials based on organic compounds (such as carbon blacks or the binding medium of the paint), while a thicker application of a material will block more than a thinner one. This allows visualisation of sub-surface features, such as abandoned or altered earlier phases (*pentimenti*), use of techniques such as superimposed forms as opposed to forms left in reserve, characteristic brushwork and so forth.

⁷ Typically, the crack bands are more broadly spaced and relate to squashing of the rolled painting.

Here, the prepared surface of the canvas is largely covered by the application of paint, which extends to the tacking margins, although small areas of ground are visible throughout the painting where forms abut. Consequently, the X-ray (**Protocol 3.6; Plates 9.a-b**) reveals a very direct rendition of form, with areas painted in reserve imaging brightly (where they block the passage of X-ray energy), with dark areas around many of these forms. The dark areas corresponding to the thinly primed areas of canvas that were left visible (i.e. unpainted; these are more X-ray transparent than heavily worked regions).

Infilling of the interstices of the threads comprising the canvas support with the priming (ground) also allows the canvas weave to be visualised in the X-ray (without the presence of the zinc containing ground, the carbon based canvas would not be resolved by the X-ray). Even if a painting is lined, making direct access to the original canvas difficult or impossible, X-ray images can permit the primary weave structure to be examined in detail. A common characterisation of canvases (apart from weave type) is the 'thread count', or number of threads per unit in warp and weft directions. Conventionally determined by hand-measuring a number of representative areas, this is now done by applying an image processing algorithm to the entire X-ray image, which has the benefit of providing both greatly enhanced determination of thread counts as well as density and thread orientation information across the whole painting (see **Protocol 3.7; Plates 10.a-c**).

The thread count on this work was determined to be 11.5 threads per centimetre in the warp direction and 8.1 in the weft. The well-distributed and even cusping distortion around the edges of the canvas suggests that the painting retains its original format.

C. Sampling and analysis

C.1 Introduction

Samples were taken of the support, ground preparation and paint layers of the work for analysis by different means in order to determine the range of materials (canvas, pigments, binders and coatings) used in the painting, the nature of the preparation layer and the sequence of layering employed in building up the painting (**Table App.1.i and Plate 14**).

To this end, a series of 12 locations selected over a representative range of the painting were micro-sampled for identification of the pigments (**App.2.i**), with five micro-samples of paint taken for analysis of the binding media (**Tables App.2.ii-2.iv**). Two further samples were taken for preparation as cross-sections to study the layering in the selected areas, with the aim of elucidating the development of the painting (**Plates 15-19**). Finally, canvas threads were taken for fibre identification (**App.2.v, Protocol 2.7**) and radiocarbon dating (**App.2.vi, Protocol 2.8**).

Micro-samples for analysis were taken from locations that were adjudged to be original (that is, were clearly contiguous with those below and adjacent to them, and not retouching or repair). Locations were also further selected to represent as wide a range of the colours – and therefore probably pigments and media – as possible. Thus, the materials identified and discussed below



therefore represent, as far as can be determined, the full extent of the original palette used by the artist.

The micro-samples taken for pigment characterisation were subjected to systematic analysis by polarised light microscopy (PLM) combined with UV-visible-near infrared micro-spectrophotometry, scanning electron microscopy-energy dispersive X-ray spectrometry (SEM-EDX) and Raman microscopy and some Fourier Transform Infrared Spectroscopy-Attenuated Total Reflectance (FTIR; **App.2.i-2.ii; Protocols 2.1-2.4**).

Organic components were identified by FTIR (**App.2.ii, Protocol 2.4**) and subsequently by Gas Chromatography-Mass Spectrometry (GCMS; **App.2.iii; Protocol 2.5**). Protein staining of cross-sections using SYPRO[®] Ruby was also conducted (**App.2.iv, Protocol 2.6**).

All of the analytical techniques applied are standard methods within the field, capable of allowing the kinds of differentiation required for this type of work. Comparison was also made between samples from the painting and examples of similar pigments from a large collection of reference standards previously analysed by multiple means⁸. Certain differentiations cannot necessarily be made from this range of techniques, although for present purposes the level of discrimination is thought to be largely or wholly sufficient. All materials were generally identified through a combination of the techniques applied; however, certain key diagnostic features were specifically determined through one or other method.

C.2 Support

The canvas was identified as being based on linen (*Linum usitatissimum* L.) in both warp and weft directions (**App.2.iv, Protocol 2.7**).

C.3 Radiocarbon dating

Radiocarbon dating was applied to fibres from the canvas support (**App.2.vi, Protocol 2.8**).

The radiocarbon date was determined as 172 years b.p. \pm 23 years. After calibration, this yielded a date distribution for which the most relevant period for the origin of the canvas lies post-1918 at the 95.4% probability level, though pre-dating the so-called ‘bomb-pulse’ period that begins in the mid-1950s.

C.4 Ground

The ground (Sample [2]) was found to be composed primarily of a lead carbonate hydroxide type white in large masses (**Plates 15-19**) combined with a small amount of finely particulate calcium

⁸ The pigment reference collection belongs to the Pigmentum Project (see: <http://pigmentum.org>) and runs to around 3500 samples of both historical and modern origin. Analysis of this collection includes PLM and SEM-EDX as well as other techniques such as X-ray diffraction and Raman microscopy. Access to this research collection is gratefully acknowledged. Reference to specific specimens in the text of this report is to the Pigmentum collection number [Pxxxx]. An organic binding media reference collection is also held by AA&R; samples in this set are cited as [AARxxx].

carbonate. The ground is bound in a drying oil. The light staining for protein (obtained by means of treatment with SYPRO[®] Ruby) detected in association with this layer may suggest the presence of a minor component of proteinaceous material (**App.2.iv, Plate 16**).

C.5 Underdrawing

No underdrawing was detected.

C.6 Paint layers: Pigments

The following pigments (**Tables App.2.1, App.2.2**) were identified:

- Zinc oxide ('zinc white')
- Lead carbonate hydroxide ('lead white')
- Calcium carbonate, calcite type
- Mercury(II) sulfide ('vermillion' red)
- Lead chromate ('chrome yellow')
- Ultramarine, synthetic (blue)
- Iron hexacyanoferrate(II) ('Prussian blue')
- Copper acetate arsenite ('emerald green')
- Chromium oxide hydrate with chromium borate ('viridian' green)
- A carbon-based black

C.7 Paint layers: Binding media

All samples, including both ground and paint layers, indicated the presence of a drying oil (**App.2.ii-iii**); in the white paint, specifically linseed oil Sample [4]; in a yellow paint either walnut oil or a mixture of linseed and poppy oil Sample [6].

Additionally, staining of a cross-section of Sample [7] with SYPRO[®] Ruby indicated that the white paint probably contains a protein (**App.2.iv, Plate 16**).

FTIR also indicated the presence of metal soaps, probably of lead and zinc, assumed to be reaction products between pigments and binding medium (**App.2.ii**).

C.8 Stratigraphy

The preparation of cross-sections allowed for examination of the overall stratigraphy and composition of the priming and paint layers.

In Sample [7], from an area of pink-red, the white ground layer contains masses of compact lead white with a more translucent surrounding material. The white area above this, based on zinc white, is of a distinctly different composition and appears to be partially mixed into the pink-red (vermillion and zinc white) layer above.

Sample [9], a blue from the sky, similarly shows some dense masses of lead white in the ground layer. Above this is a blue and white layer based on ultramarine and zinc white, with streaks of darker blue running through it.

In both cases the primary paint layers show significant wet-in-wet mixing of colours.

D. Discussion of the findings

D.1 Support, ground and preparatory work

D.1.i The support

The painting has been executed on a plain-weave, linen canvas (**Plates 5, 6, 11**), which preserves its selvedge edge along the uppermost and lowermost tacking margins (**Plate 11.c**). The weave features a double warp (two threads) and single weft structure with threads in both directions spun with a z-twist (**Plate 11.a**), with thread counts of 11.5 per cm in the warp direction and 8.1 per cm in the weft direction (see **Plate 10**). The weave is quite tight, with only occasional, small interstices found between the threads. Two dyed warp threads (a dark, bluish brown tone) are incorporated in the looming close to the selvedge edge on both sides of the canvas, providing an additional visual indicator of the edging (**Plate 11.b**). Due to the fact that the selvedge is preserved on both sides of the canvas, it is possible to state the measurement for the width of the textile, approximately 73.5 cm. A similar finding of blue threads was noted in the support of a Larionov painting dated to 1909, *Natur morte aux soucis et plante grasse*, in the collection of the Musée national d'art moderne, Paris. Here, the two sets of blue stripes (a thicker one, with a thin stripe to each side) are positioned in a manner so that they divide the width of the textile, rather than being set along the edges as found in *Tiraspol Landscape*⁹.

The canvas is of a rather rough aspect, suggesting it is not high quality. This is seen by the inclusion of many slubby and irregular threads (with a z-twist aspect) in both directions of the weave, as well as numerous bits of linen fibre husk (**Plate 11.a**), indicating that the plant fibres were not carefully cleaned and homogenized before processing as threads. The type of material is more consistent with those produced for domestic or industrial use, rather than canvas produced specifically for fine art painting.

The canvas is unlined, so the verso is fully visible (**Plates 5, 6**). It is affixed to a later (non-original) stretcher, primarily by means of round-headed tacks, that appear to follow the original tacking points to a high degree (**Plates 11.b, 11.c**). As noted, the canvas selvedge is preserved along the tacking margins on the top and bottom. In some areas, the tacking margins may be seen to extend around the 2 cm thickness of the stretcher (**Plate 11.b**) while in others they are a bit thinner (**Plate 11.c**).

⁹ Illustrated: Rioux, Aitken and Duval (1995) *op. cit.* p. 26. Discussed: Rioux, Aitken and Duval (1998) *op. cit.* p. 18.

The stretcher appears to be of the same dimensions as the original version (80 x 95.5 cm, bars 7 cm in width), as no noticeable change in dimensions of the painting may be discerned and no cracking associated with an earlier stretcher bar of different dimensions was observed. This is confirmed by the even cusping features found around the edges of the canvas (**Plate 10.a**). The inscriptions and labels present on the verso date to after the painter's death¹⁰.

D.1.ii Priming

The canvas has been primed with a white ground layer, that appears to have been applied to the stretched canvas by hand, as it conforms to the painting surface but does not extend over the tacking margins (**Plates 11.b, 11.c**). Its application is thin and irregular; it does not always fill the interstices between the canvas threads (which are small, as the weave is quite tight), which are often barely covered by the white application (**Plates 12.a, 12.b**). It exhibits a granular aspect, which seems to be a result of a very coarse grade of lead white pigment, including large white agglomerates, which are surrounded by a smaller amount of finely ground calcium carbonate (see cross-sections, **Plates 15-19**). It is possible that a low-grade quality of lead white was bought specifically for preparation of the canvas, as the distinctive large white masses seen in the ground here do not appear in the paint proper.

D.1.iii Underdrawing

No clear evidence for the use of either underdrawing or underpainting was detected in the examination of the painting, nor in the infrared images that were taken (**Plates 7, 8**).

D.2 Paint, pigments and binding media

D.2.i General observations

The condition of the painting is generally quite good, although there is minor loss and flaking, predominantly along the upper and lower edges (clearly visible in the UV image: **Plate 2**). As noted above, although it is on a new stretcher, it retains its original dimensions.

Both the canvas and the ground might be seen in the context of an artist interested in working on a textured ground, and/or, an artist wanting to save money on supplies. The canvas - likely a cloth made for domestic or industrial use, not as an artists' canvas - and the lead white used in the ground - granular and coarsely ground - may both have been a cheap source of needed materials. Equally, as the ground is clearly applied by hand - this is not a factory prepared, ready to use painter's canvas - less cost was likely incurred through the choice to mix the lead white and oil and applying the mixture as part of the process of creation. There is no evidence for the application of the ground onto the tacking edges; it extends only to the edges of the image plane. Another piece of evidence that may attest to the artist in savings mode is found in the occasional occurrence of brush hairs in the paint; well-crafted brushes in good

¹⁰ These are described in more detail in Franken (2017a) *op. cit.*

condition generally do not lose hairs, while poor quality, or older well used ones are prone to shed. Such inclusions are, however, not excessive, and do not form obvious visual feature.

The granular aspect of the lead white, the inclusion of slubby fibres and plant husks all provide the painter with a textured, irregular surface on which to paint. Given the use of wide brushes, evident brushstroke and little concern for smooth transitions and blending, this effect is well suited for the aesthetic of the work.

The painting is executed in a very sure and spontaneous manner apparently without an underdrawing, suggesting that the shapes were roughly laid in as the artist progressed the composition. The prepared surface of the canvas is largely covered by the application of paint, which extends to the tacking margins, although small areas of ground are visible throughout the painting where forms abut. No evidence for complex layering was seen; areas are worked quite directly, with mixing both on the palette, and wet-in-wet directly on the canvas. The colours are bright and intense, the paint strongly opaque and used quite thickly as well as spread thinly in other passages. No use of transparent glazes were observed; the colours remain intense, though the surface aspect is quite matte. The painting does not show evidence of having been varnished, in keeping with the artist's preference for a brightly coloured, rough, matte finish.

D.2.ii Paint: pigment and binding medium

The painting displays a marked vertical crack pattern, particularly visible in both raking light and in the 3D surface scan (**Plates 3, 4, 13**). This effect could have been caused by the painting being rolled, after it has substantially dried; there is a report available which describes that artworks in Goncharova and Larionov's studio were deposited rolled, after their deaths, or, on an earlier occasion¹¹. However, rolling cracks are usually more irregular and broadly spaced; these are quite tight and even, and extend from selvedge to selvedge (as is also seen in other paintings examined, such as *The Jewish Family*). Thus, this possibility must be left as an open question though the cracking seems more likely to be a result of the stresses within the canvas, than of former storage conditions.

The palette used in this work is quite limited in scope, with more or less one pigment sufficing to render a specific colour, apart from the blues and greens where two of each has

¹¹ Chauvelin, J. 'Témoignages/ Encounters', *InCoRM Journal*, vol.1 Nos. 2-3 (2010) pp. 6-11, esp. pp. 8, 9. On their 'return to Paris in 1915, Goncharova and Larionov brought with them hundreds of works rolled up in their luggage in view to future exhibitions in Europe'. It is also known that after their deaths, Alexandra Tomilina-Larionova (Michal Larionov's widow) did not have the means to pay the rent for the studio on the rue Jacques Callot where the artists had lived and worked since the 1020s, and where many artworks were stored. Chauvelin describes the chaos of the studio, noting that paintings were stored both flat or rolled. 'Their works were piled and stacked, totally cluttering this studio – which, in fact, was quite large – with dozens of portfolios full of hundreds (if not thousands) of drawings, watercolours, gouaches, sketches. Oils on cardboard or canvases were lying either flat or were rolled up. [...] The warehousemen started taking the packets and boxes down and loading them into the trucks rather carelessly. [...] Two days later everything had been taken away and deposited randomly in the storage rooms at the two Paris warehouses, for which Tomilina was never able to pay. All these works disappeared from sight for the next thirty years. [...] A small number of works selected by Tomilina (only those by Micha) were taken from the studio to the third floor of the apartment on the rue Jacques Callot, which was already full to bursting.'

been employed (synthetic ultramarine and Prussian blue; emerald and viridian greens). To create the various hues of the landscape, the blues, greens, yellow and white have been combined to allow for a range of tones.

Observation of the verso of the canvas reveals a darkening of the fibres that relates to broad areas of the composition (**Plate 5**). This would suggest that some passages of paint were quite medium rich, and the priming quite porous, allowing for the penetration of the oil binder to the verso of the art work. This is likewise in agreement with the fact that no obvious isolation layer of glue or oil was observed as the first step in preparation of the canvas; the white ground would appear to have been applied directly to the woven support.

The cross-sections prepared confirm the observations made on the surface, and with the various forms of imaging: the paint was worked freely and directly (**Plates 15-19**). Mixing has taken place both on the palette, and on the brush, sometimes wet-in-wet directly on the canvas. This direct application has led to quite thin passages where the canvas weave and lumpy texture of the ground remain fully visible, and others where it is fully obliterated by a heavy build-up of impasto. The fields of colour are delineated from one another by dark contours, which were primarily added as the final program of working.

D.2.iii Materials analysis and implications for dating

A date of 1905 is proposed for the painting; this is not wholly supported by the radiocarbon analysis, which suggests a somewhat later date. Due to this slight discrepancy, a second sample is being tested to strengthen the results of this analysis. The report will be adjusted accordingly.

The radiocarbon measurement of the fibre of the canvas gave a date for its harvesting (prior to manufacture into thread, and subsequently into canvas) post-1918 at the 95.4% probability level, though pre-dating the so-called 'bomb-pulse' period that begins in the mid-1950s. In addition to this a period of 3-5 years typically needs to be allowed for processing of raw plant fibre into canvas and its subsequent use by the artist (comprising: drying, processing to fibre, spinning to thread, weaving to canvas, sales and transport to merchant, purchase and use by artist). This would suggest a later date of origin for the painting, more likely 1921-23, although the radiocarbon result should ideally be reconfirmed before formally re-dating the work.

The materials identified in the painting (pigments and binding media) would not however otherwise be incompatible with the supposed date (although they also continued in use after that time) and would not preclude a revision of date consistent with the radiocarbon result. The findings generally agree well with the data collected in the study of 45 paintings by Goncharova and Larionov in the collection of the Musée national d'art modern, Paris¹².

¹² The ground presents the single exception, in that only grounds based on zinc white were noted in those examples prepared by the artists themselves. Rioux, Aitken and Duval (1998) *op. cit.* p. 18.



Other technical characteristics arising from the larger review of the works of Goncharova and Larionov may also contribute to a fuller understanding of the relative dating of this painting in the future.

E. Conclusions

The examination of the painting revealed a work that was created with great spontaneity, with a limited palette of materials to create a vivid depiction of a sunlit landscape. The textured aspect of the support and ground are particularly characteristic and are mirrored in the brushwork and handling of the paint. The date of the work might be reconsidered in light of the radiocarbon analysis, which suggests a dating in the early 1920s (this is in the process of being reconfirmed, by running a second sample, at the date of writing); the inscriptions on the verso of the painting some of which may relate to shipping between Russian and France, and their relationship to those on other works, should also be considered.



F. Acknowledgements

Art Analysis & Research would like to thank the following people for their contributions:

Museum Ludwig

Dr Yilmaz Dzewior	Director, Museum Ludwig	
Rita Kestring	Deputy Director, Museum Ludwig	
Petra Mandt	Deputy Head of Conservation, Museum Ludwig	Project coordinator Paintings conservator

Project Team, AA&R

Dr Jilleen Nadolny	Principal Investigator	Project management
Dr Nicholas Eastaugh	Chief Scientist	Materials and data analysis
Bhavini Vaghji	Senior Scientist	Materials analysis
Francis Eastaugh	Senior Imaging Engineer	Scientific imaging processing
Dr Joanna Russell	Scientist	Materials analysis

Project Subcontractors

Verena Franken	Freelance paintings conservator, Cologne, Germany	Project coordinator, examination, documentation and archival research
Patrick Schwarz	Rheinisches Bildarchiv Köln, Cologne, Germany	Photographic documentation
Prof. Hans Portsteffen, Andreas Krupa	Department of Conservation, Cologne University of Applied Sciences, Germany	Capture of X-ray data
Xavier Aure-Calvet	Freelance imaging specialist, Bristol, UK	3D imaging capture and post processing
Prof Haida Liang and team	Nottingham Trent University, UK	Hyperspectral imaging
Dr Irka Hadjas and team	ETH/ Swiss Federal Institute of Technology, Zurich, Switzerland	Radiocarbon analysis

We would also like to extend our sincere thanks to the Peter and Irene Ludwig Foundation and to the RARP donors and to its board of trustees, without whose generosity and vision this project would not have been possible.

G. Appendices

Standard protocols used by AA&R in the preparation of this report for sampling, materials analysis and imaging are listed in each subsection below and detailed in the appendices to the global summary report.

App.1 Sampling and sample preparation

Protocols:

[P.1.1] Sampling

[P.1.2] Cross-sectional analysis

App.1.i Sampling

#	Colour	Description	Location ¹³	Analysis
1		Blue	542/697	PLM, SEM-EDX, Raman
2		White ground	41/521	PLM, SEM-EDX, Raman, FTIR
3		Green	91/122	PLM, SEM-EDX, Raman, FTIR,
4		White	197/409	PLM, SEM-EDX, Raman, FTIR, GCMS
5		Purple	196/388	PLM, SEM-EDX, Raman
6		Yellow	337/245	PLM, SEM-EDX, Raman, FTIR, GCMS
7		Pink-red	1/318	PLM, SEM-EDX, Raman, CSA, SYPRO® Ruby staining
8		Light brown	504/405	PLM, SEM-EDX, Raman
9		Blue	552/705	Raman, CSA
10		Dark blue	602/514	PLM, SEM-EDX, Raman

¹³ The coordinates in this column are given in millimetres, the measurements taken from the left edge of the picture, and from the lower edge of the picture.

#	Colour	Description	Location ¹³	Analysis
11		Mid-yellow	627/409	PLM, SEM-EDX, Raman
12		Black	148/462	PLM, SEM-EDX, Raman
13		Mid-green	2/257	PLM, SEM-EDX, Raman, FTIR
14		Canvas fibre	n/a	Fibre identification, FTIR, C14

App.1.ii Cross-sectional analysis

Results are illustrated in **App.5, Plates 15-19**.

App.2 Materials analysis summary results

Protocols:

- [P.2.1] Polarised light microscopy (PLM)
- [P.2.2] Scanning electron microscopy-energy dispersive X-ray spectrometry (SEM-EDX)
- [P.2.3] Raman microscopy
- [P.2.4.1] Fourier Transform Infrared Spectroscopy-Attenuated Total Reflectance (FTIR-ATR)
- [P.2.5] Gas Chromatography-Mass Spectrometry (GCMS)
- [P.2.6] Protein staining with Sypro Ruby©
- [P.2.7] Fibre Identification
- [P.2.8] Radiocarbon dating

App.2.i SEM-EDX, Raman microscopy and PLM analysis

#	Colour	SEM-EDX (elements)			Raman Microscopy (peaks, cm ⁻¹)	Identification
		Major	Minor	Trace		
1	Blue	-	Na, Al, Si, S, Zn	<i>K, Ca, Pb</i>	581 (vw), 547 (m)	Ultramarine Zinc oxide
2	White ground	Pb	Ca	<i>Al, Si</i>	1363 (vw, br), 1050 (m), 679 (vw), 406 (vw, br), 125 (vw, sh), 109 (s)	Lead carbonate hydroxide [P0864]
					1086 (vw), 1050 (w), 407 (vw, br), 281 (vw), 127 (vw, sh), 110 (m)	Lead carbonate hydroxide (main) Calcium carbonate, calcite type (minor)

Table App.2.i Analytical results SEM-EDX, Raman Microscopy and PLM

#	Colour	SEM-EDX (elements)			Raman Microscopy (peaks, cm ⁻¹)	Identification
		Major	Minor	Trace		
3	Green	-	Na, S, Cl, Cr, Zn	<i>Mg, Al, Si, K, Ca, Cu, As, Sr¹⁴, Ba, Pb</i>	-	Chromium oxide hydrate Zinc oxide Barium sulfate Zinc potassium chromate hydrate (probable) Copper acetate arsenite (trace)
4	White ¹⁵	Zn	Pb	<i>Al, Si, S, Ba</i>	1049 (w), 437 (vw), 110 (m)	Zinc oxide (main) Lead carbonate type white (minor)
					1437 (vw), 1302 (vw), 1049 (w), 437 (vw), 253 (vw) , 109 (m)	Zinc oxide (main) Lead carbonate type white (minor) Mercury sulfide (trace)¹⁶
5	Purple	-	Na, Al, S, Zn	<i>Mg, Si, P, Cl, K, Ca, Pb</i>	544 (vw)	Ultramarine Zinc oxide
6	Yellow	Pb	Al, S, Cr	<i>Si, Ca, Zn</i>	1054 (vw), 971 (vw), 842 (vs), 403 (vw), 377 (w), 360 (s), 338 (vw), 328 (vw), 139 (vw)	Lead chromate yellow [P2238] Lead carbonate type white
7	Pink-red	Zn	S, Hg	<i>Al, Si, Pb</i>	343 (w), 285 (vw), 253 (vs), 143 (vw), 107 (vw)	Mercury sulfide [P0010] Zinc oxide
8	Light brown	-	Al, Zn	<i>Na, Mg, Si, P, S, Ca, Cr, Fe, Pb</i>	1592 (vw, br), 1291 (vw, br), 840 (vw)	Carbon-based black Lead chromate
					1594 (vw, br), 1295 (vw, br), 841 (vw), 547 (vw)	Carbon-based black Lead chromate Ultramarine Zinc oxide
10	Darker blue	-	Na, Al, Si, S, Zn	<i>Mg, Cl, K, Ca, Cr, Ba</i>	545 (w), 257 (vw)	Ultramarine
					1590 (vw, br), 1295 (vw, br), 664 (vw), 547 (w)	Ultramarine Carbon-based black Zinc oxide
11	Mid-yellow	Zn	Mg, Al	<i>Si, S, Ca, Cr, Ba, Pb</i>	1052 (vw), 1048 (vw), 841 (m), 435 (vw), 403 (vw), 376 (vw), 360 (w), 339 (vw), 329 (vw), 253 (vw), 139 (vw, sh), 113 (w)	Lead chromate yellow [P2238] Lead carbonate type white Zinc oxide Mercury sulfide¹⁷

¹⁴ Probably associated with the barium sulfate.

¹⁵ Red and blue pigment particles were visible in the white matrix.

¹⁶ Mercury was not identified in the SEM-EDX analysis.

¹⁷ As note 16, above.

Table App.2.i Analytical results SEM-EDX, Raman Microscopy and PLM						
#	Colour	SEM-EDX (elements)			Raman Microscopy (peaks, cm ⁻¹)	Identification
		Major	Minor	Trace		
12	Black	-	Na, Al, Si, Ca	Mg, P, S, Cl, K, Cr, Zn, Ba, Hg, Pb	1592 (w, br), 1307 (w, br), 545 (w), 253 (vw)	Carbon-based black Ultramarine Mercury sulfide
13	Mid-green	-	Al, S, Ca, Zn, As	Na, Si, Cl, K, Cr, Cu, Ba, Pb	843 (vw), 544 (vw)	Ultramarine Lead chromate
					947 (vw), 840 (vw), 539 (vw), 489 (vw), 370 (vw), 322 (vw), 243 (vw), 216 (m), 172 (w), 153 (m), 119 (m)	Copper acetate arsenite [P1302]

App.2.ii Fourier Transform Infrared Spectroscopy-Attenuated Total Reflectance (FTIR-ATR)

Table App.2.ii Summary results from FTIR			
#	Colour	FTIR (peaks, cm ⁻¹)	Identification
2	White ground	3536 (vw), 3284 (vw, br), 2954 (vw), 2918 (vw), 2849 (vw), 1795 (vw), 1732 (vw), 1646 (w), 1537 (vw), 1514 (vw), 1392 (vs), 1152 (vw), 1088 (vw), 1043 (m), 872 (m), 847 (vw), 763 (vw), 753 (vw, sh), 712 (vw), 679 (m)	Lead carbonate hydroxide [P0864] Calcium carbonate, calcite type ¹⁸ Protein Oil Metal soap formation
3	Green	2926 (vw), 2853 (vw), 2098 (w), 1732 (s), 1434 (vw), 1358 (vw), 1263 (vw), 1053 (vw), 1005 (vw), 837 (vw), 795 (vw), 782 (vw), 731 (vw)	Iron hexacyanoferrate(II) Chromium borate ¹⁹ Binding media component (type unidentified) ²⁰ Carbonate ²¹
4	White	3531 (vw), 3377 (w, br), 2918 (m), 2851 (w), 1734 (m), 1717 (vw), 1648 (vw), 1576 (vw, sh), 1559 (m), 1541 (s), 1456 (vw, sh), 1398 (vs), 1364 (vw, sh), 1321 (w), 1244 (vw, sh), 1163 (vw), 1117 (vw), 1092 (vw), 1045 (w), 983 (vw), 681 (s)	Lead carbonate hydroxide Barium sulfate Oil Metal soap formation, zinc-based ²² Metal soap formation, presumably lead-based

¹⁸ The very strong peak present at 1392 cm⁻¹ is shared by both lead carbonate hydroxide and calcium carbonate, calcite type.

¹⁹ The peaks assigned to chromium borate are present in the reference spectrum of chromium oxide hydrate, reference number P0092.

²⁰ The three peaks present are peaks assigned to the binding medium however from these three peaks it is unclear what the binding medium is as there are multiple binding media's which show these mentioned peaks such as oils, alkyds and natural resins to name a few.

²¹ It is not possible to say in which form the carbonate is since both lead carbonate type white and calcium carbonate show this peak. Other peaks which can be used to differentiate one from the other are absent.

Table App.2.ii Summary results from FTIR			
#	Colour	FTIR (peaks, cm⁻¹)	Identification
6	Yellow	3392 (vw, br), 2951 (vw, sh), 2916 (s), 2849 (s), 1738 (w), 1716 (vw), 1592 (vw), 1547 (s), 1529 (vs), 1454 (s), 1398 (m), 1165 (vw), 1098 (w), 1068 (vw), 1049 (w), 969 (vw), 852 (m), 833 (vw), 824 (vw, sh), 781 (vw), 743 (w), 719 (w), 677 (vw), 624 (w)	Lead chromate [P2238]²³ Oil Metal soap formation, zinc-based ²⁴ Metal soap formation, presumably lead-based
13	Mid-green	3524 (vw), 3397 (vw), 3381 (vw, br), 2954 (vw, sh), 2918 (s), 2849 (m), 1739 (w), 1616 (vw), 1590 (vw), 1549 (vw, sh), 1539 (s), 1454 (s), 1410 (vw), 1398 (w), 1375 (vw, sh), 1164 (vw, sh), 1114 (vw, sh), 1073 (s), 1052 (vw, sh), 983 (vw), 874 (vw), 816 (w), 764 (m), 722 (vw), 688 (vw), 667 (vw), 635 (m), 606 (vw)	Copper acetate arsenite [P1302] Barium sulfate Calcium sulfate, gypsum type Calcium carbonate, calcite type Oil²⁵ Metal soap formation, zinc-based²⁶

²² The peaks present in the sample spectrum matched the reference spectrum of zinc stearate, reference number AAR308. Zinc was identified in the SEM-EDX analysis.

²³ The reference spectrum of lead chromate consists of peaks corresponding to lead sulfate too. These peaks are also present in the sample spectrum which could suggest that the lead chromate is likely in the form of lead chromate sulfate or lead sulfate is present in the reference spectrum too. The SEM-EDX data of the sample showed high amounts of lead with minor amounts of chromium and sulfur.

²⁴ The peaks present in the sample spectrum matched the reference spectrum of zinc stearate, reference number AAR308. Zinc was identified in the SEM-EDX analysis.

²⁵ The characteristic peak of oil occurring at around 1160 cm⁻¹ was not observed in the spectrum due to the presence of barium sulfate whose peaks were masking this characteristic peak of oil however it is assumed that oil is present due to the formation of metal soaps.

²⁶ The peaks present in the sample spectrum matched the reference spectrum of zinc stearate, reference number AAR308. Zinc was identified in the SEM-EDX analysis.

App.2.iii. Gas Chromatography-Mass Spectrometry (GCMS) Analysis

Table App.2.iii. Summary results from GCMS					
Sample #	Hexadecanoic acid, methyl ester (C ₁₇ H ₃₄ O ₂)		Octadecanoic acid, methyl ester (C ₁₉ H ₃₈ O ₂)		Ratio
	Retention time, mins	Peak area	Retention time, mins	Peak area	
4	25.655	1.162 x 10 ¹⁰	29.583	8.805 x 10 ⁹	P/S = 1.32
6	25.664	2.507 x 10 ⁹	29.607	9.315 x 10 ⁸	P/S = 2.69

The P/S value of **Sample [4]**, white paint, was 1.32, consistent with **linseed oil**.

The P/S value of **Sample [6]**, yellow paint, was 2.69, consistent with **walnut oil or a mixture of linseed and poppy oil**. Other non-traditional examples could be safflower or soybean oil.

App.2.iv SYPRO[®] Ruby protein staining

Table App.2.iv. SYPRO [®] Ruby stain results for 955.A, Sample [7] ²⁷ .				
Layer	EDX	FTIR	SYPRO [®] Ruby stain	Interpretation
Ground	Pb Ca Al, Si	Peaks for protein and oil	Very faint pink coloration in bright white areas of ground	Light pink tone indicates possible small amount of protein
Paint	Zn S, Hg, Al, Si, Pb	n.a.	White paint is clearly pink-stained. Mixed pink/white layer has overall pink colour (stain harder to detect in purely pink paint areas)	Protein in white paint, and possibly red

App.2.v. Canvas fibre identification

Table App.2.v. Canvas fibre identification, Sample [14]		
Sample	Observations	Interpretation
Vertical	Colourless to yellow fibres with high birefringence. Nodes across fibres, parallel extinction, S-twist, 2-6 divisions wide (at 40x)	Bast fibre, probably linen (<i>Linum usitatissimum</i> L.)
Horizontal	Nodes across fibres, parallel extinction, S-twist, 2-6 divisions wide (at 40x)	Bast fibre, probably linen (<i>Linum usitatissimum</i> L.)

²⁷ For the ground layer, EDX and FTIR data derives from separate analysis of another sample.



App.2.vi. Radiocarbon measurement

Radiocarbon dating is a method for determining age estimates of formerly living organic materials²⁸. Carbon has three naturally occurring isotopes, ^{12}C , ^{13}C and ^{14}C . Both ^{12}C and ^{13}C are stable, but ^{14}C decays by very weak beta decay to nitrogen (^{14}N) with a half-life of approximately 5,730 years. While alive, organic materials continue to exchange carbon with the environment, such that they are in equilibrium. On death, the ^{14}C component begins to decay, such that over time the relative amount decreases. Measuring the level of ^{14}C remaining in the material then allows for a date to be estimated. This must be additionally calibrated against natural historical variation in relative ^{14}C levels in the environment, for which there are accepted standard curves expressing the changes over time²⁹.

Prior to radiocarbon measurement, fibre identification was undertaken and the canvas sample was pre-tested using FTIR to ascertain the presence of any contaminating material that could influence the outcome. As noted elsewhere, the fibre was identified as a bast type, probably linen (*Linum usitatissimum* L.). FTIR indicated the presence of *poly*(vinyl acetate), and possibly an oil, in addition to the cellulose of the fibre³⁰.

The canvas sample was then submitted to the Laboratory of Ion Beam Physics, ETHZ at the Swiss Federal Institute of Technology (*Eidgenössische Technische Hochschule Zürich*) for radiocarbon dating (see **Protocol 2.7**).

²⁸ Based on from the websites of the NDT Resource Center, <http://www.ndt-ed.org/EducationResources/CommunityCollege/Radiography/Physics/carbondating.htm> and the website of the Oxford Radiocarbon webinfo site: <http://c14.arch.ox.ac.uk/embed.php?File=webinfo.html>, both consulted on 3 February 2013.

²⁹ For example, that used here is one known as IntCal13.

³⁰ Sample pre-treatment aims to remove non-cellulosic materials prior to the radiocarbon measurement.

Table App.2.vi. Radiocarbon measurement										
Sample-Nr.	Sample Code	Material	C14 age BP	±1σ	F14C	±1σ	δC13 ‰	±1σ	mg C	C/N
ETH-77067	AAR0955.A 14	Textile fibre	172	23	0.9788	0.0028	-26.7	1	1	169.09

The radiocarbon date was determined as 172 years b.p. ±23 years. After calibration, this yielded a date distribution for which the most relevant period for the origin of the canvas lies post-1918 at the 95.4% probability level, though pre-dating the so-called ‘bomb-pulse’ period that begins in the mid-1950s. [NOTE: This result is being checked by means of running a second sample; the report will be updated accordingly]

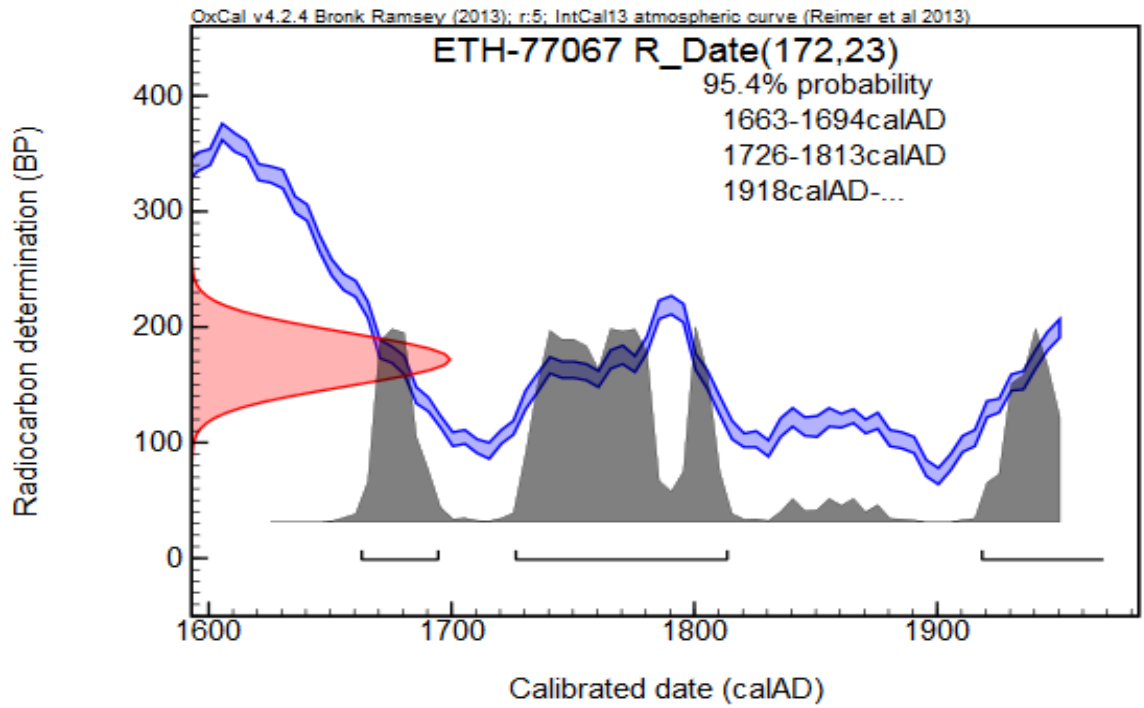


Figure App.2.vi. Radiocarbon determination.



App.3 Imaging methods

Protocols:

- [P.3.1] Photography with visible light
- [P.3.2] Photography with ultraviolet illumination
- [P.3.3] 3D laser surface mapping
- [P.3.4] SWIR infrared imaging (IR)
- [P.3.6] X-radiography
- [P.3.7] Thread counting and weave analysis

App.4 Plates



Plate 1. Natalia Goncharova, Paysage de Tiraspol (Tiraspol Landscape), 1905, collection Museum Ludwig: Inv. Nr. ML 01483. **Recto, visible light.**

Rheinisches Bildarchiv Köln, Patrick Schwarz, rba_d050882_08, www.kulturelles-erbe-koeln.de/documents/obj/05021025



Plate 2. Natalia Goncharova, Paysage de Tiraspol (Tiraspol Landscape), 1905, collection Museum Ludwig: Inv. Nr. ML 01483. **Recto, UV light.**

Rheinisches Bildarchiv Köln, Patrick Schwarz, rba_d050882_06, www.kulturelles-erbe-koeln.de/documents/obj/05021025



Plate 3. Natalia Goncharova, Paysage de Tiraspol (Tiraspol Landscape), 1905, collection Museum Ludwig: Inv. Nr. ML 01483. **Recto, oblique illumination.**

Rheinisches Bildarchiv Köln, Patrick Schwarz, rba_d050882_04, www.kulturelles-erbe-koeln.de/documents/obj/05021025



Plate 4. Natalia Goncharova, Paysage de Tiraspol (Tiraspol Landscape), 1905, collection Museum Ludwig: Inv. Nr. ML 01483. **Recto, 3D laser scan.**

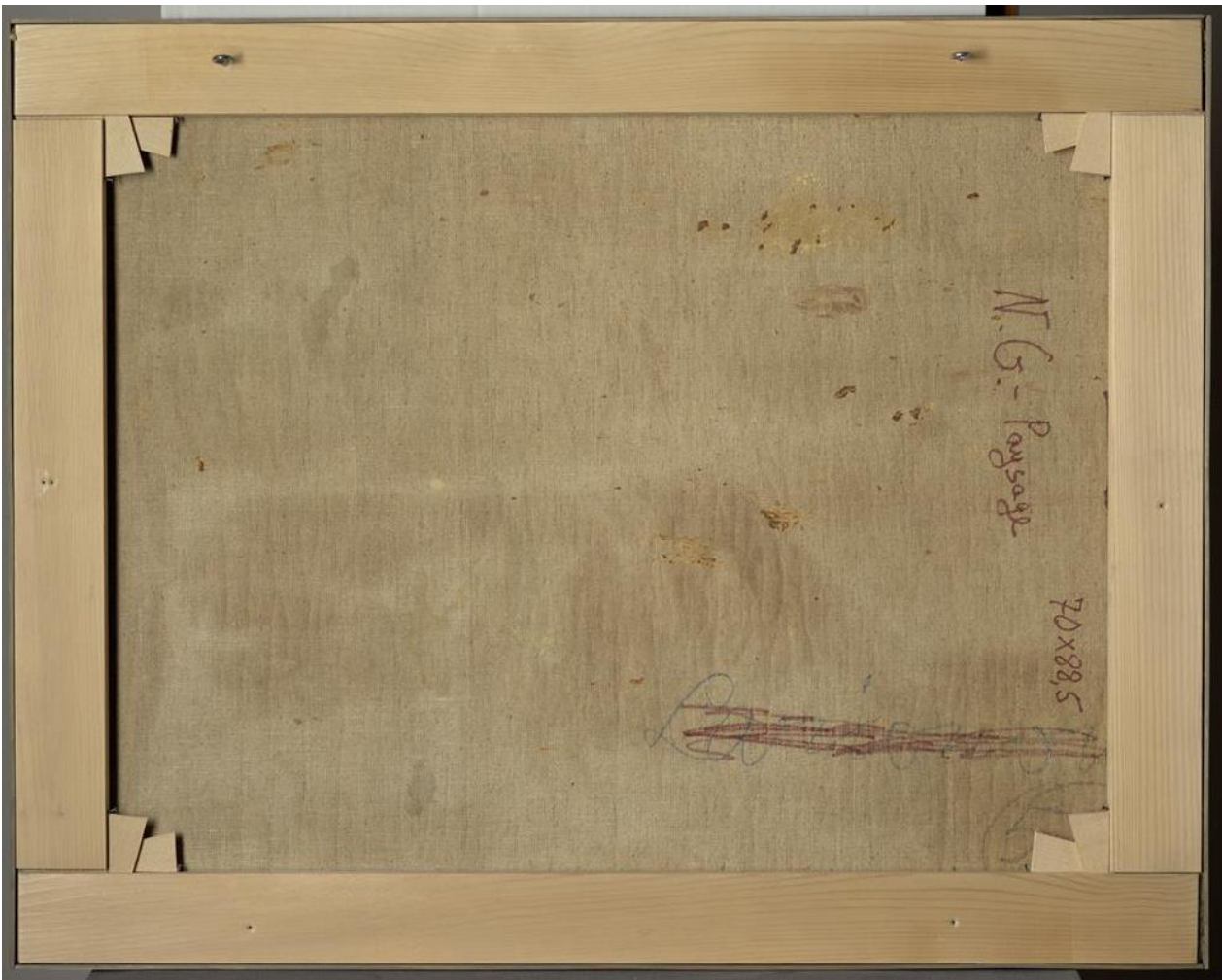


Plate 5. Natalia Goncharova, *Paysage de Tiraspol* (Tiraspol Landscape), 1905, collection Museum Ludwig: Inv. Nr. ML 01483. **Verso, visible light.**

Rheinisches Bildarchiv Köln, Patrick Schwarz, rba_d050882_02, <http://www.kulturelles-erbe-koeln.de/documents/obj/05021025>

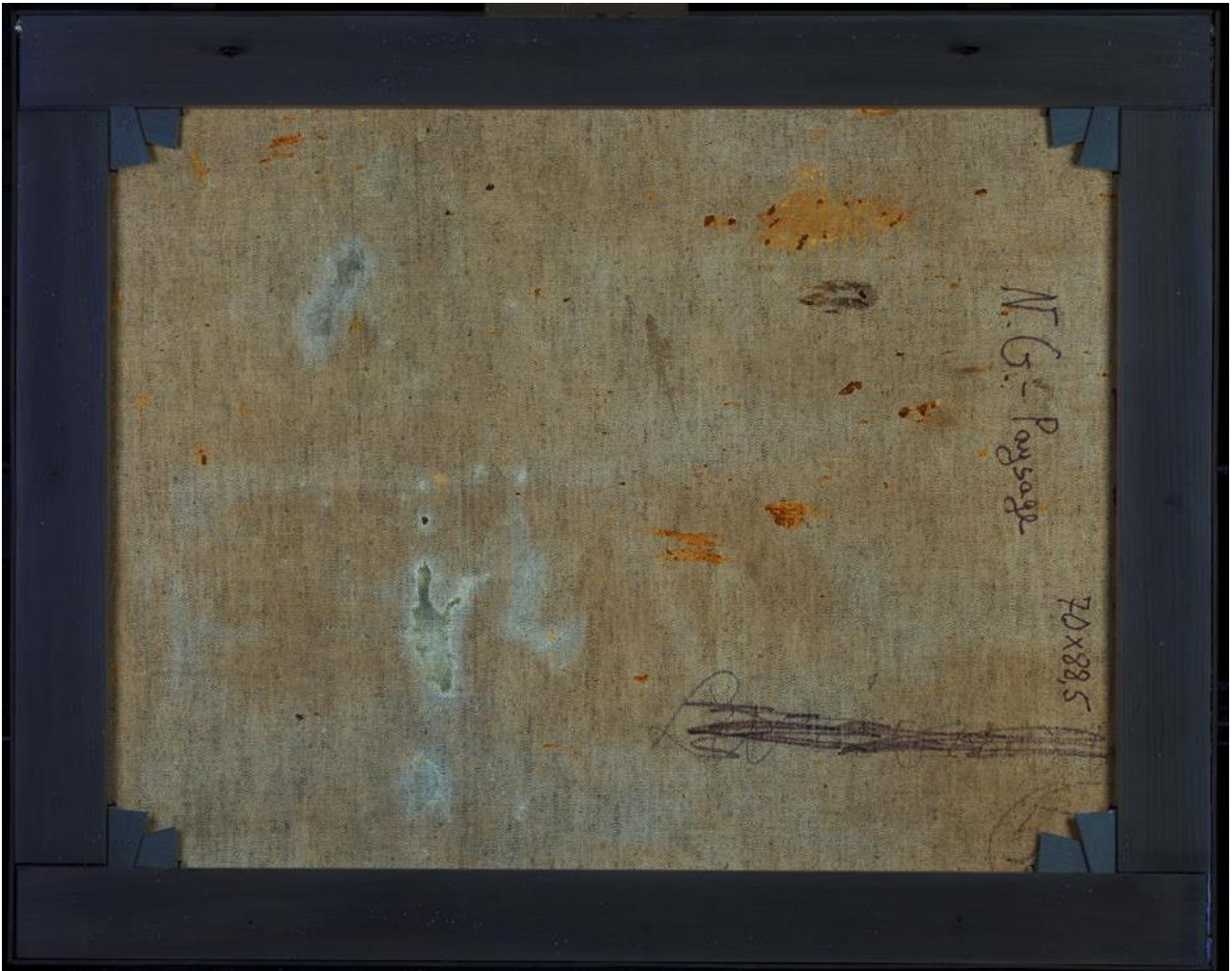


Plate 6. Natalia Goncharova, Paysage de Tiraspol (Tiraspol Landscape), 1905, collection Museum Ludwig: Inv. Nr. ML 01483. Verso, **UV light**.

Rheinisches Bildarchiv Köln, Patrick Schwarz, rba_d050882_07, www.kulturelles-erbe-koeln.de/documents/obj/05021025

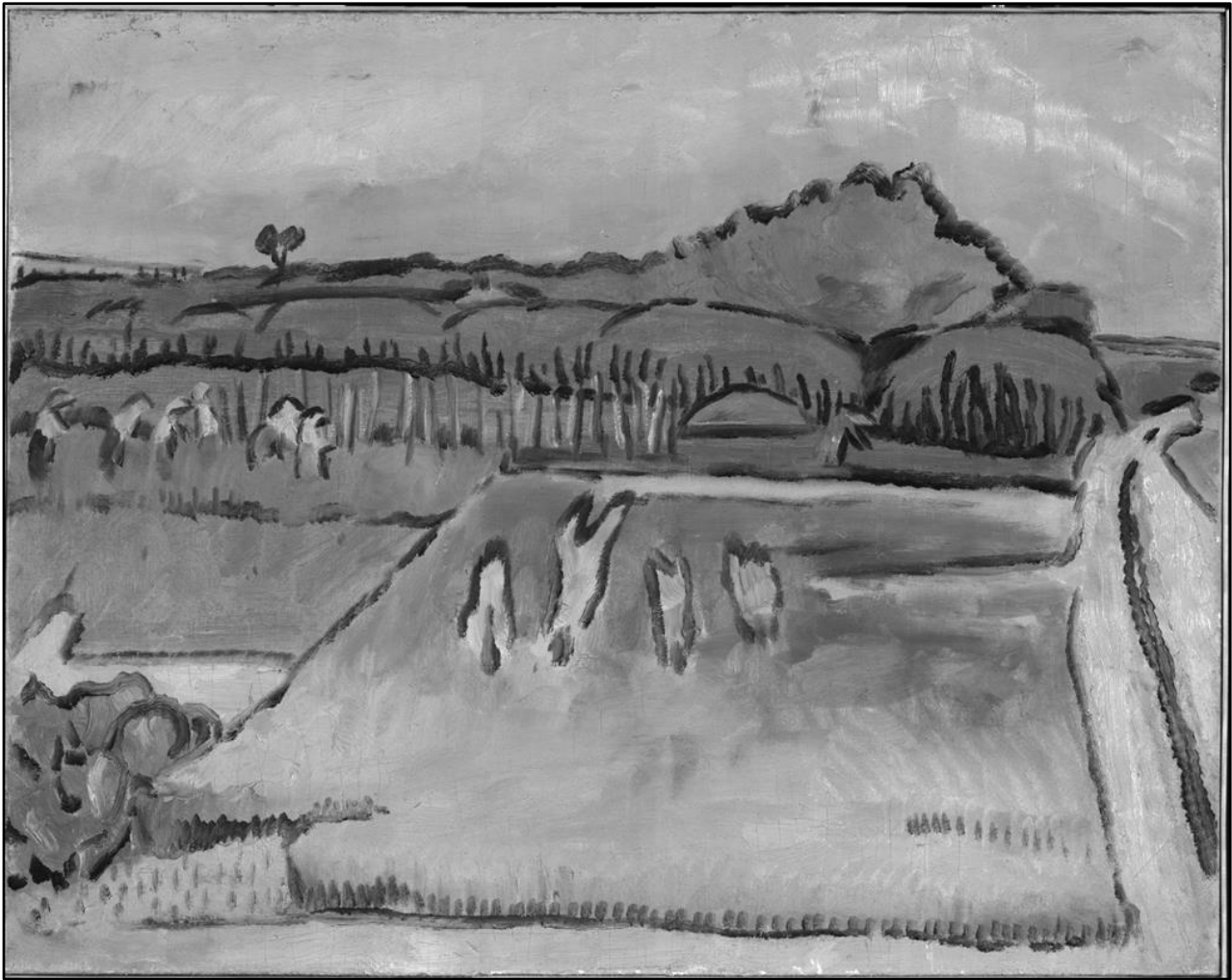


Plate 7. Natalia Goncharova, Paysage de Tiraspol (Tiraspol Landscape), 1905, collection Museum Ludwig: Inv. Nr. ML 01483. **Recto, SWIR image.**

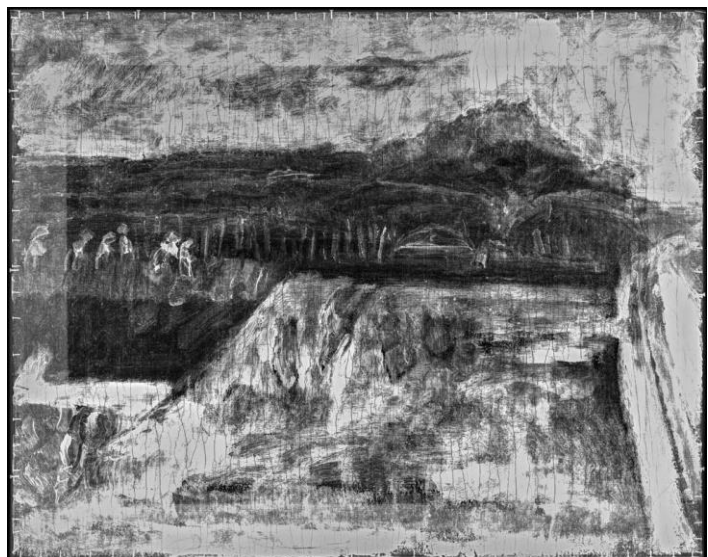


Plate 8. Natalia Goncharova, *Paysage de Tiraspol (Tiraspol Landscape)*, 1905, collection Museum Ludwig: Inv. Nr. ML 01483. **Recto, SWIR image, detail.** No underdrawing or pentimenti are visible; instead the thin, free nature of the brushwork may be seen.



Plate 9.a Natalia Goncharova, Paysage de Tiraspol (Tiraspol Landscape), 1905, collection Museum Ludwig: Inv. Nr. ML 01483. **X-ray image.**

Plate 9.b The X-ray image before digital compensation for the stretcher bars.



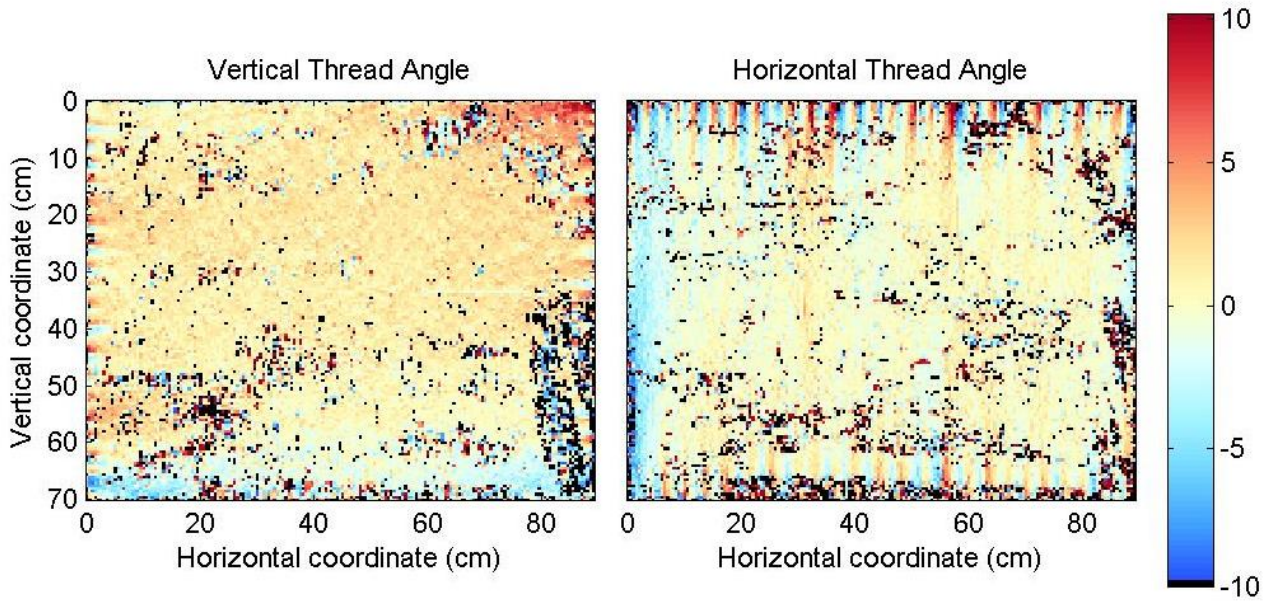


Plate 10.a Maps showing variation in canvas thread angle.

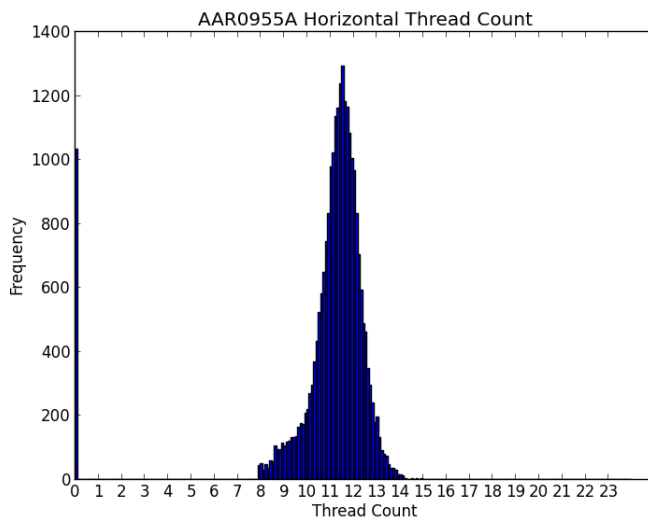


Plate 10.b Histogram of horizontal thread (in this case related to the warp) count readings.

Showing variation in thread count per centimetre.

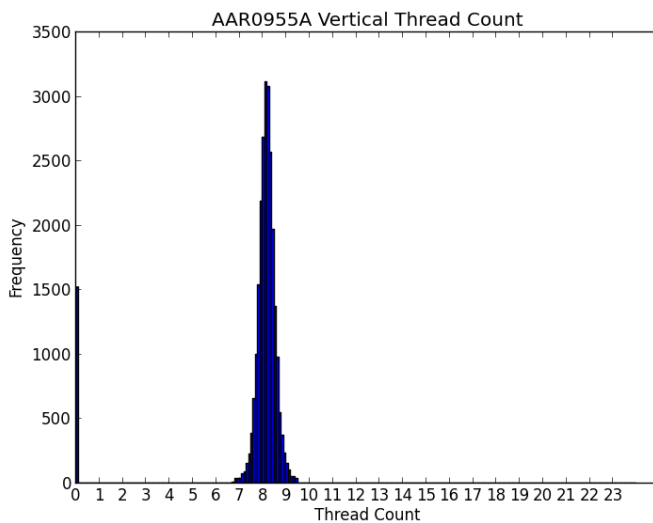


Plate 10.c Histogram of vertical thread count readings (in this case related to the weft).

Showing variation in thread count per centimetre.

Plate 10.d Table of thread count data (threads per centimetre)		
	Mean	Estimated thread count (mode)
Warp (horizontal)	11.35	11.5
Weft (vertical)	8.17	8.1



Plate 11.a Detail of canvas, verso.

The weave is a double warp, single weft, with a double warp blue strip (as below) running along the selvedge. The fibre is a bast type, probably linen (*Linum usitatissimum* L.).



Plate 11.b Detail of canvas, right tacking margin, showing selvedge, right, along top edge.

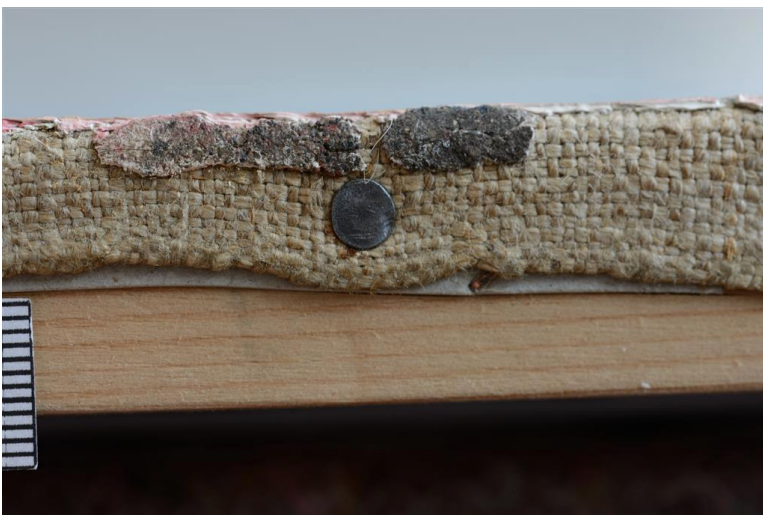


Plate 11.c Detail of canvas, bottom tacking margin, showing selvedge.

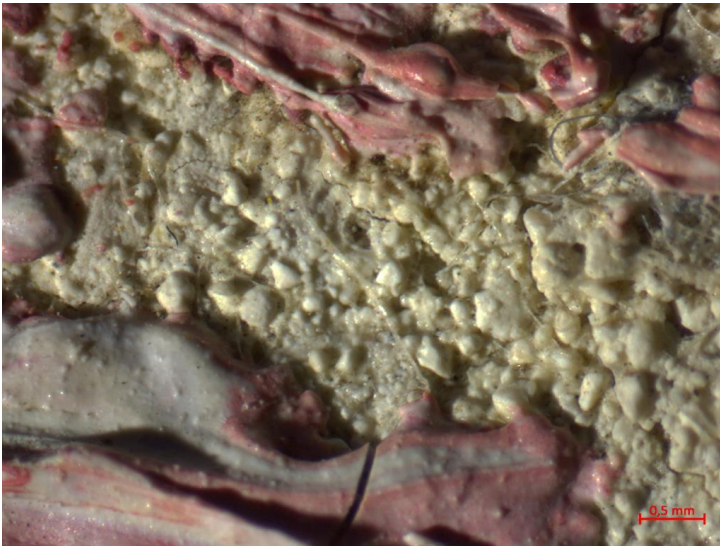


Plate 12.a Macro detail of the lead white-based priming on the canvas, recto.

Shows the granular aspect of this layer.



Plate 12.b Higher magnification of the ground, as above.



Plate 12.c Detail of cracks in the painting, showing the effect of the granular ground on the paint surface.



Plate 13.a Macro detail, showing brushwork with a brush loaded with several colours.

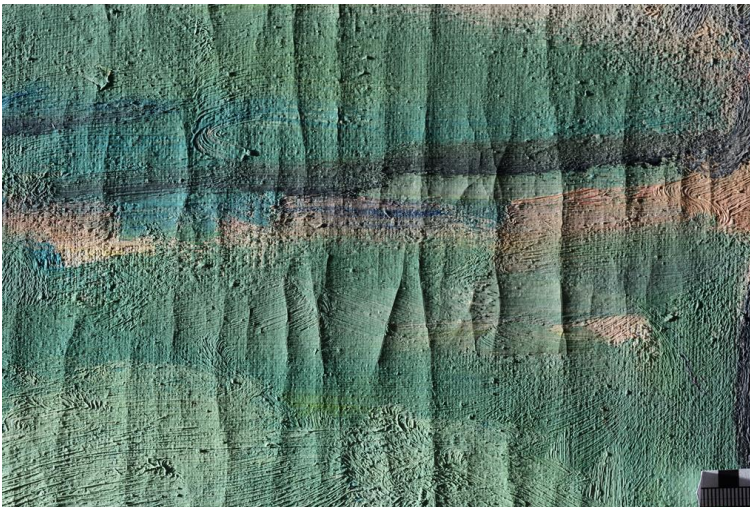


Plate 13.b Detail of surface texture.

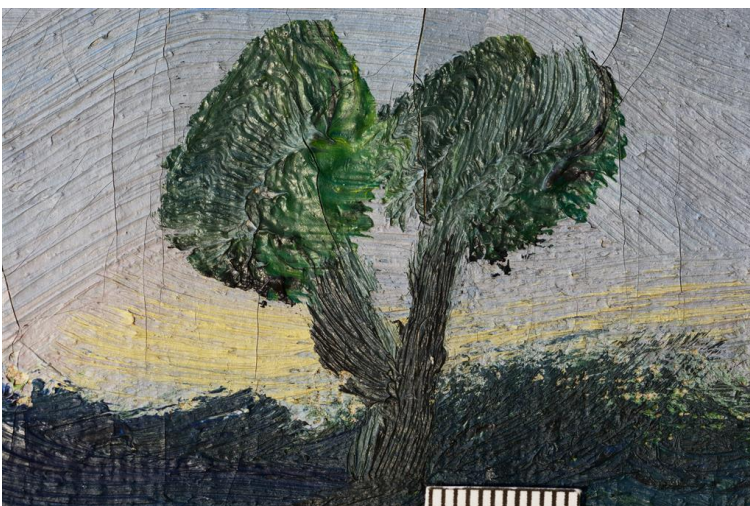
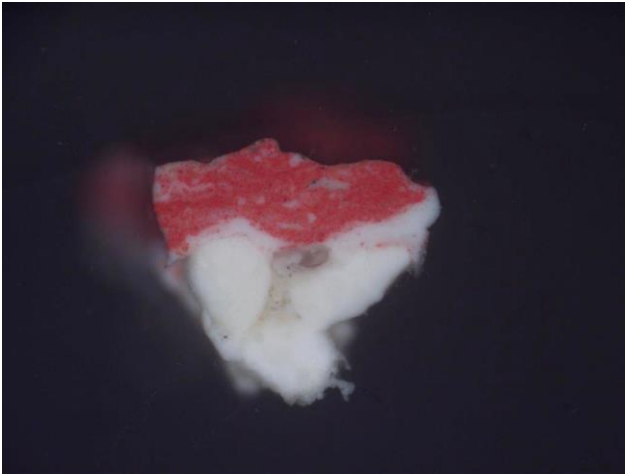


Plate 13.c Macro detail of a tree, background. Paint applied wet over dry.

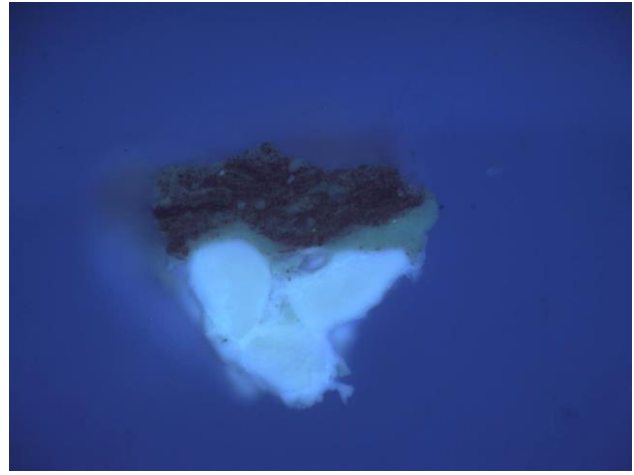


Plate 14. Image showing approximate location of samples taken for materials analysis.

App.5 Cross-sections³¹



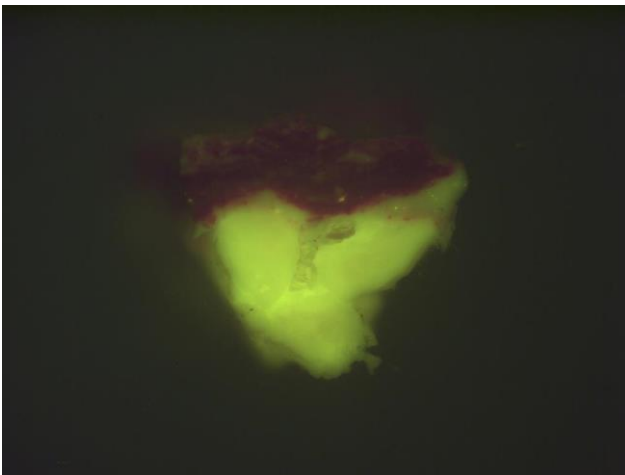
a.



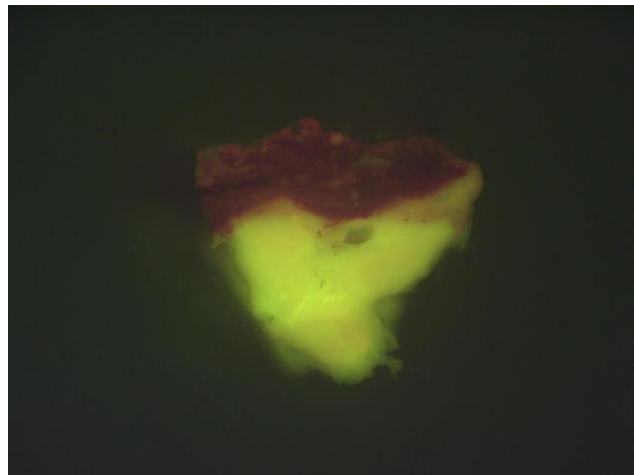
b.

Plate 15. Cross-section, Sample [7].

Image ~1mm high. Pink-red. The white ground layer appears to contain masses of compact white lead with more translucent surrounding material. The white layer above this (zinc white; dull yellow in the UV image, right) is of a distinctly different composition, as seen in the UV image, and appears to be partially mixed into the pink-red (vermilion and zinc white) layer above.



a.



b.

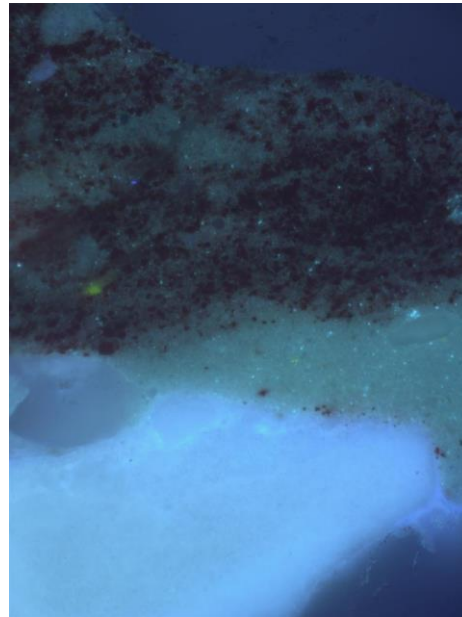
Plate 16. Cross-section, Sample [7], stained with SYPRO[®] Ruby.

Image ~1mm high viewed with Leica I3 filter before (left) and after (right) staining. Very faint pink coloration is notable in bright white areas of ground, while the white paint is clearly pink-stained. The mixed pink/white layer has overall pink colour, although the stain is harder to detect in pink paint areas. This result suggests the presence of a protein in the white paint and probably some minor quantity in the ground as well.

³¹ Photographed under visible light, left (a.), and with ultraviolet illumination, right (b.), unless otherwise stated.



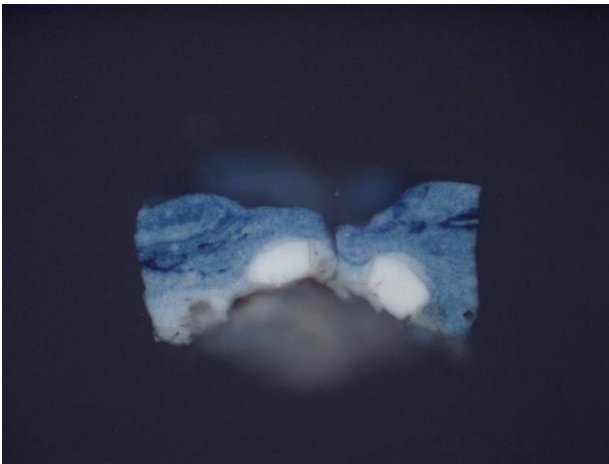
a.



b.

Plate 17. Cross-section, Sample [7].

Image ~260 μ m high. Detail at higher magnification showing the mixed red and white paint, including a few blue-green particles.



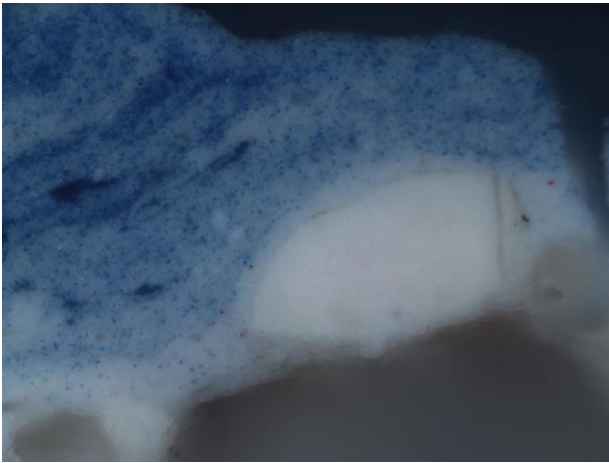
a.



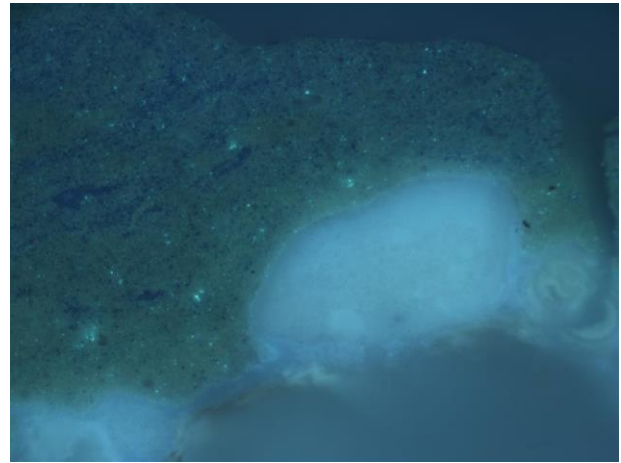
b.

Plate 18. Cross-section, Sample [9].

Image ~1mm high. Blue from sky. As in sample [7], some dense masses of lead white can be seen in the ground layer. Above this is a blue and white layer (ultramarine and zinc white) with streaks of darker blue running through it.



a.



b.

Plate 19. Cross-section, Sample [9].

Image ~260 μ m high. Blue from sky, detail at higher magnification. Fine particles with a green luminescence can be seen throughout the blue layer in the UV image, characteristic of zinc oxide ('zinc white'). The large white masses consist of lead carbonate hydroxide. The thin, greyish white material under and around the large lead white masses is calcite.